Impact on stellar properties of changing physics
SAC Summer School Report

Nathalie Themessl
Max Planck Institute For Solar System Research

Jason A. Drury
University of Sydney

Zsolt Keszthelyi
University Observatory Munich

30.09.2014

Contents

1 Introduction

1.1 Motivation

Stellar evolution and structure are key to our understanding of astrophysics. Theoretical stellar evolution calculations provide the basis for determining the age and compositions of stars as well as the distances between them. These calculations are crucial for investigating the current structure of the galaxy and its formation. Furthermore, the synthesis of all elements heavier than helium is dependent on nucleosynthesis within stars. Thus, to understand the chemical history and origins of the universe, and therefore our own existence we must first understand the processes which drive stellar evolution.

Stellar modelling provides a means of testing theoretical stellar evolution calculations and our understanding of the physics behind such systems by comparing the results with observational data. This comparison allows us to refine the theoretical calculations and provides us with a greater understanding of the physics behind these phenomena as well as the possibility of predicting future observations.

1.2 MESA

Modules for Experiments in Stellar Astrophysics (`MESA`) is a 1D (open source) stellar evolution code[1]. It allows for the investigation of evolving stellar models with different initial properties including initial mass, hydrogen and helium fractions, mixing length, and rotation. In our project work we used `MESA` in order to track the evolutionary responses of changing the input physical parameters, firstly the mass and the metallicity. Thus we created different profiles, reproduced the Kippenhahn diagram and obtained Hydrogen profiles as well.

2 Hertzsprung-Russell diagram

One of the most important diagrams in stellar astrophysics is the **Hertzsprung-Russell diagram** (HRD), which provides an insight into the evolution of stars. The diagram was originally created by Ejnar Hertzsprung and Henry Norris Russell. It shows the relationship between the star's luminosity or absolute magnitude versus its effective temperature or spectral type. In general, stars of greater luminosity populate the top of the diagram, while stars with higher surface temperature are located in the left side of the diagram. Typically, all the stars in the galaxy have a different chemical composition, even though most of them are build up of elements very similar to those in our own Sun. The metallicity is characterized as the mass fraction of elements heavier than helium and can be calculated as follows:

$$Z = \sum_{i>He} \frac{m_i}{M} = 1 - X - Y, \tag{1}$$

[1] `http://mesa.sourceforge.net/`

with M as the total mass of the system, X as the hydrogen mass fraction and Y as the helium mass fraction.

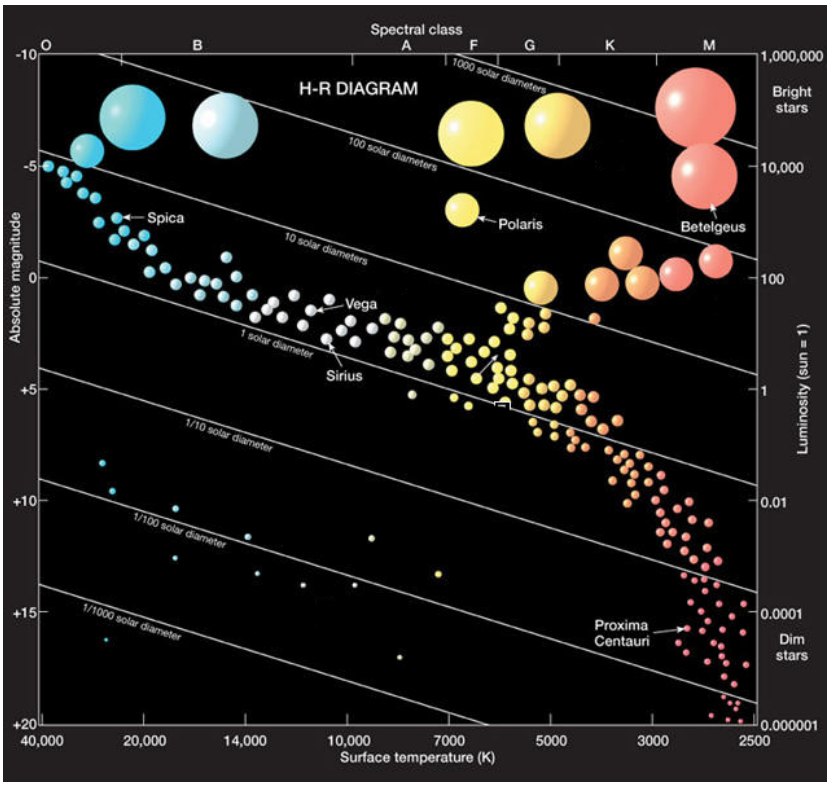

Figure 1: Hertzsprung-Russell diagram (Credit: Prentice Hall, Inc.)

As is shown in Figure 1, stars occupy certain regions of the diagram. Many stars are concentrated along a line, which is known as the main sequence. The subgiants, giants and supergiants are located above the main sequence, while the lower left side of the diagram is populated by faint white dwarfs.

3 The evolution of stars

Stars undergo a sequence of physical changes during their lifetimes, which ranges from trillions of years for low mass stars to only a few million years for the most massive stars. Due to those long timescales stellar evolution is studied by observing a wide range of stars at different points in their evolution. The supplementary compilation of computer models then allows to simulate stellar structure and evolution.

3.1 Pre-main sequence evolution

Stars form from collapsing interstellar dust clouds that break into smaller fragments. The release of gravitational potential energy and the increase of temperature and pressure lead to the formation of rotating spheres of hot gas, known as **protostars**.

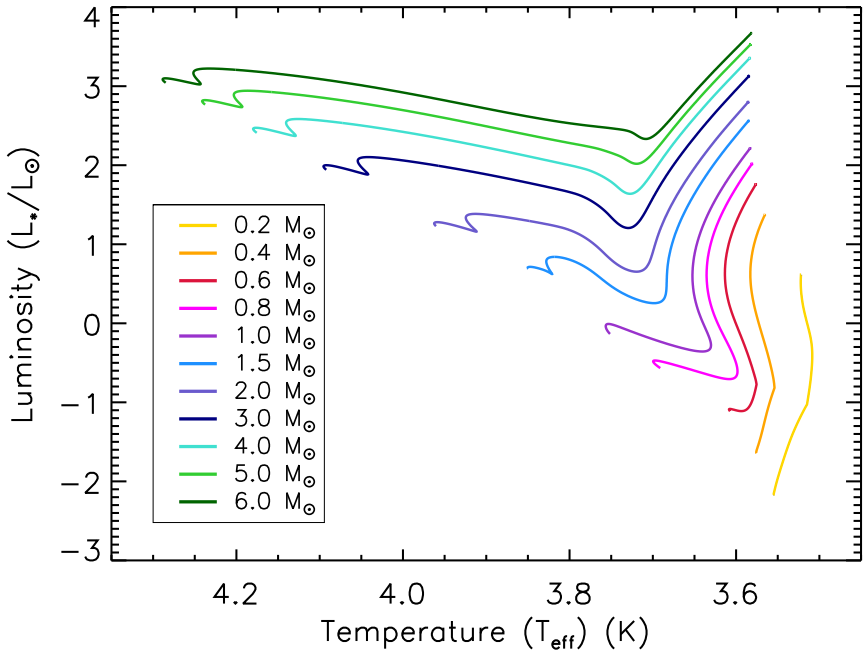

Figure 2: Pre-main sequence evolutionary tracks of stars with initial composition of $Z = 0.02$.

These stars contain primarily hydrogen, helium and very small amounts of metals that are all uniformly distributed throughout the star. At that stage of evolution, they are still embedded in the cloud of dust and gas. Consequently, a protostar is visible as a small infrared source. Further accretion onto the star disperses the cloud and it reaches its final mass. Once it becomes visible as a pre-main-sequence object, the star settles at the **stellar birthline** (see Figure 3) in the Hertzsprung-Russell diagram.

The pre-main-sequence evolutionary tracks for a sequence of masses are shown in Figure 2. As the protostar-collapse slows down, the star's luminosity decreases enormously while its effective temperature increases slightly. This stage of the evolution is visible as the nearly vertical line in the Hertzsprung-Russell diagram known as the **Hayashi track**. The shape and position of this track depends mainly on the mass and chemical composition of the star. Stars on the Hayashi track are completely convective during the first one million years of the collapse (Carroll & Ostlie , 2007). During this period the first stage of nuclear burning occurs in the stellar core once the temperatures are high enough to enable nuclear reactions. The central temperature then continues to rise and further ionisation leads to a decrease in opacity in that region. Consequently, a radiative core develops, which encompasses more and more of the star's mass. This radiative core then allows the energy to escape into the convective envelope more easily, causing the luminosity of the star to increase again. After developing a radiative zone the stars move on to the **Henyey track**. While low-mass stars have nearly vertical evolution tracks, very massive stars are directly born onto the Henyey track (Carroll & Ostlie , 2007). Moving along this track the stellar luminosity remains almost constant.

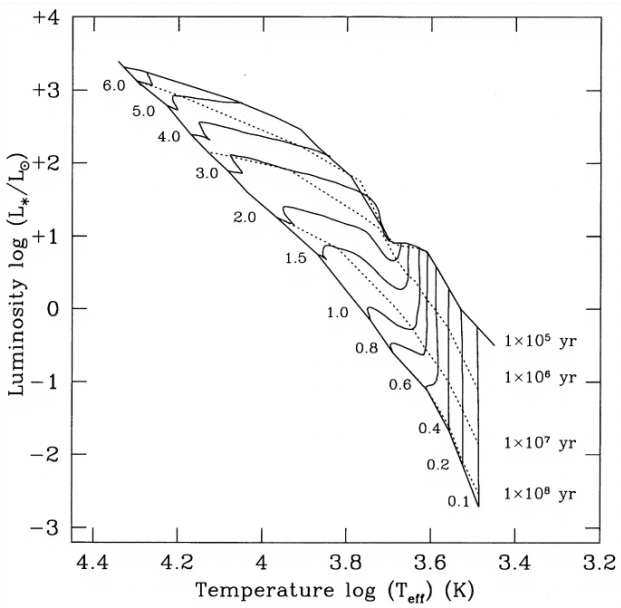

Figure 3: Theoretical PMS tracks in the HR diagram. Selected isochrones are displayed by the dotted lines. For each track, the evolution starts at the stellar birthline (right solid line), and ends at the zero age main sequence (left solid line). The number indicates the mass of the model in $M_\odot$ (from Palla et al. (1999)).

Once the energy production reaches a certain level, the central core is forced to expand. The diagonal line in the Hertzsprung-Russell diagram where stars of various masses first reach the main sequence and begin hydrogen burning is known as the **zero age main sequence** (ZAMS), which is shown in Figure 3.

For stars of less than 0.6 $M_\odot$ the upward branches are missing before they settle down at the main sequence (see Figure 2). They are very close to being fully convective and as a consequence they have no Henley track.

3.2 Main-sequence evolution

The star reaches the **main-sequence** once the core temperature is sufficiently high to enable **nuclear fusion**. As a consequence, the core releases energy that produces enough radiative pressure to prevent the star from collapsing any further. In this way, the star reaches hydrostatic equilibrium. On the main-sequence the star slowly converts the hydrogen in the core into helium. This phase of evolution ends when nearly all of the hydrogen in the core has been fused, and the star evolves off the main sequence. More massive stars burn faster and therefore have a short lifetime of just a few million years. In contrast, less massive stars reside in this evolutionary phase for hundreds of billions of years. Nevertheless, most stars are found on the main-sequence, simply because that stage of evolution requires the most time, while later phases proceed more rapidly.

Main-sequence and post-main-sequence evolutionary tracks of stars of different mass are shown in Figure 4, Figure 5 and Figure 6. A prominent feature is the so-called hook

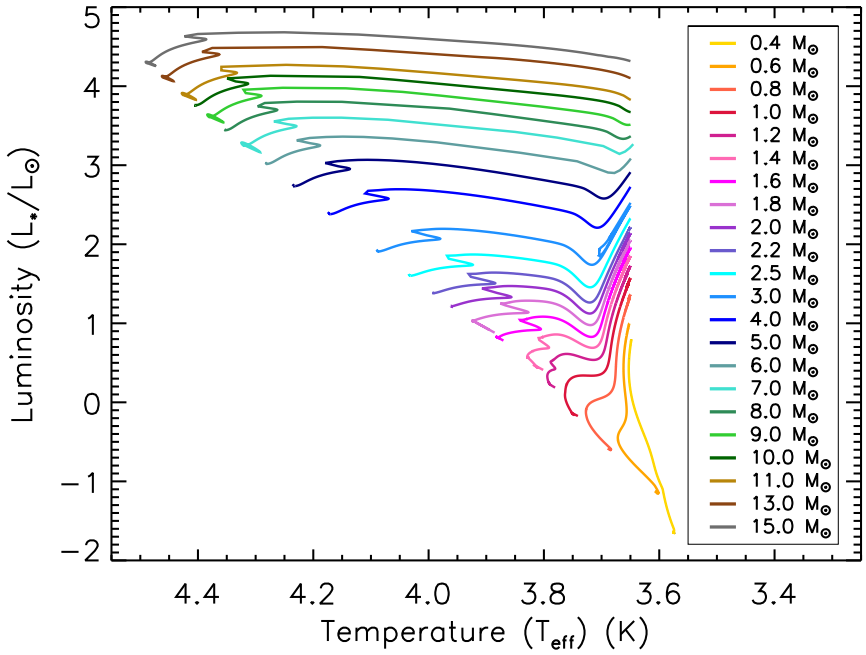

Figure 4: Main sequence evolutionary tracks of stars with initial composition of $Z = 0.02$.

which is clearly visible in the evolutionary tracks of medium and high mass stars. As the evolution on the main-sequence continues, the hydrogen in the core will be entirely depleted. Once the hydrogen abundance gets very low, an overall contraction further increases the central temperature. In the end, this effect allows to maintain the energy production and the heat in the inner center forces further nuclear fusion. Energy can then be generated in a thick hydrogen-burning shell around a small helium core. The helium core continues to grow in mass while the star moves farther to the red in the Hertzsprung-Russell diagram along the so-called **subgiant branch**. This phase ends when the mass of the core reaches a certain size that is no longer able to support the material above it.

3.3 Late stages of stellar evolution

After the exhaustion of hydrogen in the stellar core, nuclear reactions can no longer be maintained. Therefore, the core begins to contract due to its own gravity. The star then begins to burn hydrogen in a thick shell surrounding the core. The higher temperatures result in increasing reaction rates, which cause the stellar luminosity to rise by a factor of $1000 - 10.000$. In addition, the radius of the star expands greatly, which marks the **red-giant phase** of the star's life. By this time the surface of the star has cooled and it proceeds nearly vertically in the Hertzsprung-Russell diagram (see Figure 5 or Figure 6).

The evolutionary path the star takes as it moves along the red-giant branch depends on the mass of the star. For stars with less than 2 $M_\odot$ the core will become dense enough that electron degeneracy pressure will prevent it from collapsing further. In the following, the core will continue to heat until it reaches a temperature of roughly 10^8

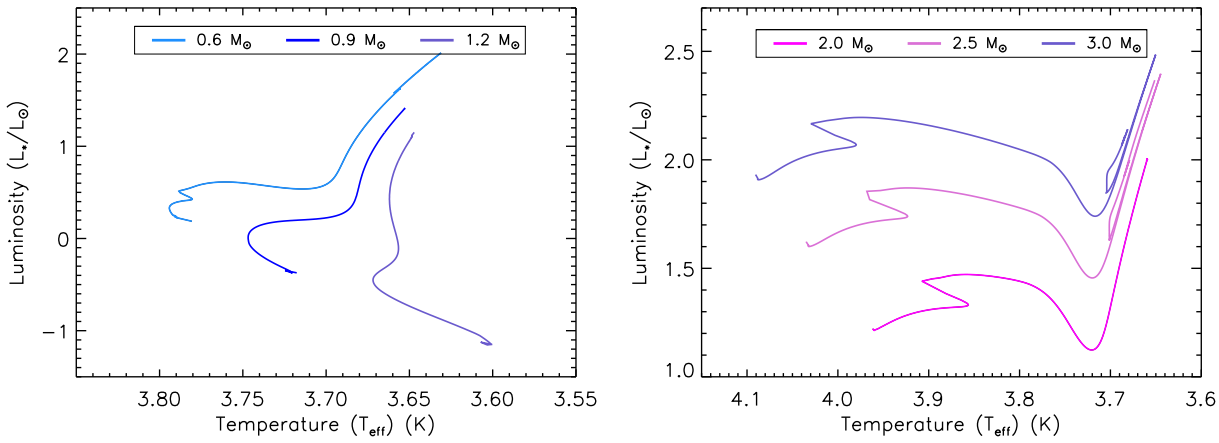

Figure 5: Main-sequence evolutionary tracks of stars with low (left panel) and intermediate (right panel) mass.

K. Then the entire core will begin to fuse helium to carbon via the triple-alpha process. The resulting energy release occurs almost explosively. However, most of the energy is absorbed by the overlying layers of the envelope, which in the end causes some mass loss. This short-lived phase of evolution of low mass stars is referred to as the **helium core flash**. In more massive stars, the collapsing core will reach 10^8 K before it is dense enough to be degenerate. Then, helium fusion will begin much more smoothly.

Once the star is fusing helium in its core, it contracts and is no longer considered a red giant. The core helium fusing phase of a star's life is called the **horizontal branch** in metal-poor ([Fe/H] ≈ -2.90, Çalışkan et al. (2014)) stars, while metal-rich ([Fe/H] ≈ 0.12, Carraro et al. (2014)) helium-fusing stars instead lie on the **red clump**.

Once the central helium is exhausted, the star collapses again, which causes helium-burning in an outer shell. At the same time, hydrogen fusion may start in a shell just outside the burning helium shell. Then the star reaches the second red-giant phase, known as the **asymptotic giant branch**. The next stages of stellar evolution depend primarily on the original mass of the star and the amount of mass loss that occurred during the star's lifetime.

At the end, the helium fusion results in the build up of a carbon-oxygen core. A star below about 8 $M_\odot$ (Carroll & Ostlie , 2007) will never start fusion in its degenerate carbon-oxygen core. Instead, the star will eject its outer layers, forming a **planetary nebula** with the stellar core becoming a **white dwarf**. The ejection of the outer mass and the creation of a planetary nebula finally ends the red-giant phase of the star's evolution. Figure 7 shows the evolution of a solar mass star with an initial composition $Z = 0.02$ from the pre-main-sequence to the white dwarf phase. In contrast, stars of higher mass may explode in **supernovaes** with their inner core collapsing into extremely dense **neutron stars** or **black holes**.

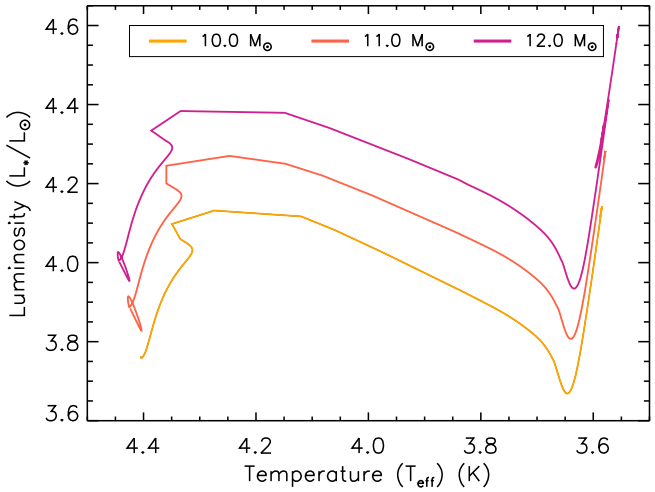

Figure 6: Main-sequence evolutionary tracks of high mass stars.

A more detailed description on stellar evolution can be found in Carroll & Ostlie (2007).

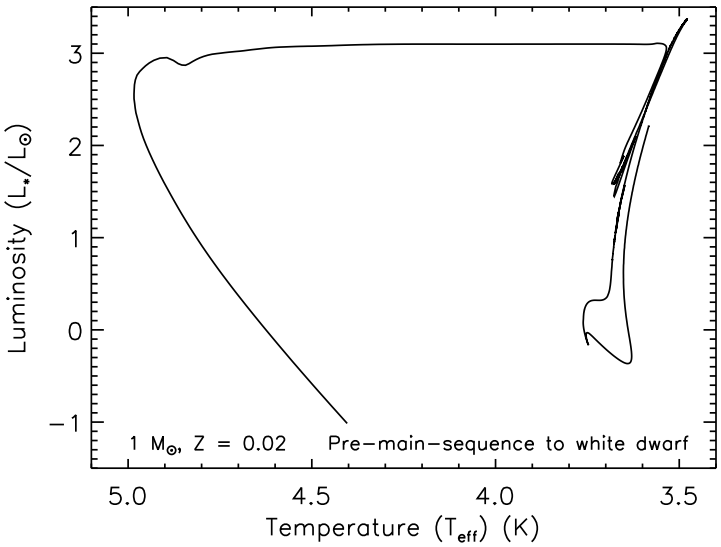

Figure 7: Evolutionary track from the pre-main-sequence to the white-dwarf phase.

3.4 Metallicity dependence

Let us begin with a fundamental equation of stellar structure, namely:

$$\frac{\mathrm{d}T}{\mathrm{d}r} = -\frac{3\kappa\rho L(r)}{16\pi acr^2T^3} \tag{2}$$

which can be derived from the radiation energy transport of a star that is in hydrostatic equilibrium (see e.g. Mihalas (1978)).

The opacity and luminosity are both altered by the metal content of the star. Since metallicity affects opacity, the behavior of the star changes and thus yields to a different evolution. This was indeed a task we showed, that changing the Z input in `MESA`, different evolutionary tracks arise.

$$\kappa \propto Z\rho T^{-3.5} \tag{3}$$

where ρ is the density and T is the temperature. Since the density and the temperature can be expressed as $\rho \propto \frac{M}{R^3}$ and $T \propto \frac{\mu M}{R}$, and using the fundamental equation of stellar structure we obtain

$$L \propto Z^{-1}R^{0.5}\mu^{7.5}M^{5.5} \tag{4}$$

where μ is the mean molecular weight and M is the total mass (Christensen-Dalsgaard (2013)). That is, the energy production and released energy weakly depend on Z, however it is far more sensitive to changes in μ.

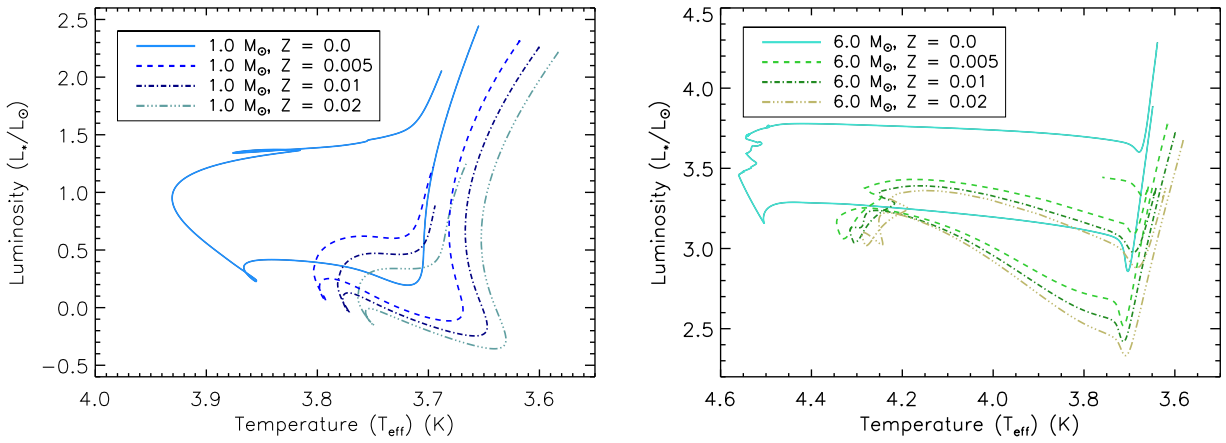

Figure 8: Pre-main-sequence and main sequence evolutionary tracks of a 1 $M_\odot$ and 6 $M_\odot$ star with an initial composition of $Z = 0, 0.005, 0.01$ and 0.02, respectively.

Figure 8 shows evolutionary tracks of stars with different initial composition of Z. The plots indicate that stars with lower initial metallicity are generally hotter. Furthermore a change in the intrinsic metallicity yields to sensitive changes in stars where the CNO cycle dominates over the pp chain. The CNO cycle becomes the major source of energy production in stars with initial masses $\approx 1.1\, M_\odot$ and core temperature slightly less than $2 \cdot 10^7$ K. The temperature gradient in stars where CNO cycle dominates drops quickly when Z is increased.

4 The Kippenhahn diagram

The Kippenhahn diagram is a detailed plot showing the structure of stellar interiors regarding their convective/radiative nature. Convection occurs when the Schwarzschild criterion is fulfilled, i.e.

$$\nabla_{rad} > \nabla_{ad} \tag{5}$$

where

$$\nabla_{rad} = \frac{\mathrm{dln}T}{\mathrm{dln}P} \tag{6}$$

and

$$\nabla_{ad} = \left(\frac{\partial \mathrm{ln}T}{\partial \mathrm{ln}P}\right)_{ad} \tag{7}$$

and, on the other hand, the radiative transport equation is defined by Equation 2. (For fully ionized gas $\nabla_{ad} = 2/5$)

The convective regions are essential for mixing and also for overshooting (see Kippenhahn & Weigert (1990)). Stellar evolution on the pre-MS are defined by the

Hayashi track and the Henyei track, respectively. The Hayashi track indicates almost fully convective behavior.

On the ZAMS the initial masses play a crucial role regarding the evolution of a star. As seen on the Kippenhahn diagram, below 0.5 $M_{\odot}$ the star are fully convective. Sun-like stars have radiative cores and convective envelopes. This is indeed the reason why the granular solar surface can be seen, convection alters the solar surface and leads to observable features. Around 1.1 $M_{\odot}$ a transient region appears, where stars have convective cores, a radiative layer and a convective surface. More massive stars do not posses convective surface any more.

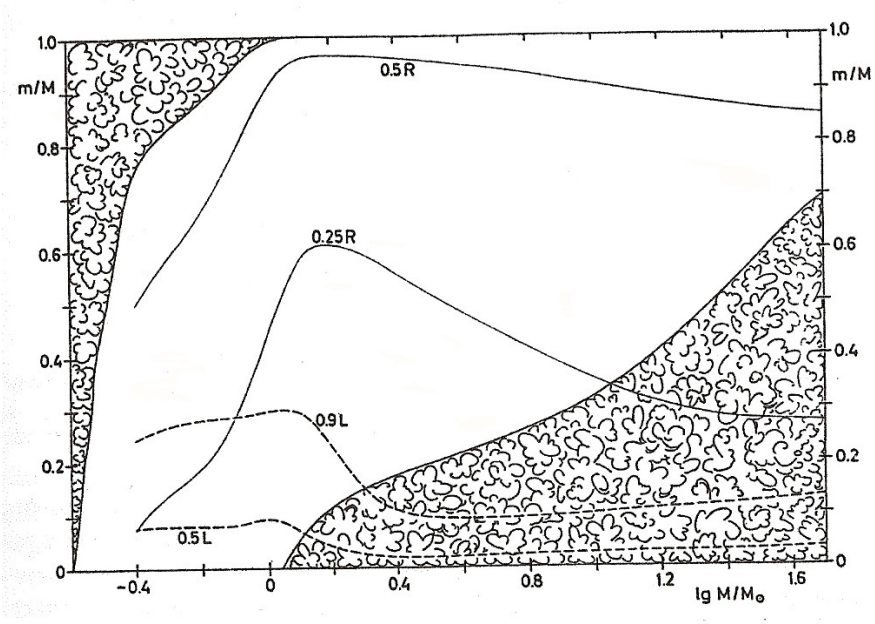

Figure 9: The Kippenhahn diagram from Kippenhahn & Weigert (1990). Cloudy parts indicate convective regions.

Using `MESA`, the evolution of 30 stars with different masses were calculated in order to reproduce the Kippenhahn diagram at the ZAMS but also to plot the TAMS.

The results show excellent agreement with the original Kippenhahn diagram. Differences are due to i) the lower resolution and ii) different numerical treatment by `MESA` (see e.g. the instrument papers, Paxton et al. (2011) and Paxton et al. (2013)).

The TAMS represents a different evolutionary stage, and it is evident that since H core burning stops, internal changes happen inside a star. The reproduced Kippenhahn diagram at the TAMS shows that the convective regions at this stage are reduced and radiation dominates. The nature of stars, however does not change, Sun-like and smaller stars have radiative cores and convective envelopes, while massive stars still have convective cores and radiative envelopes.

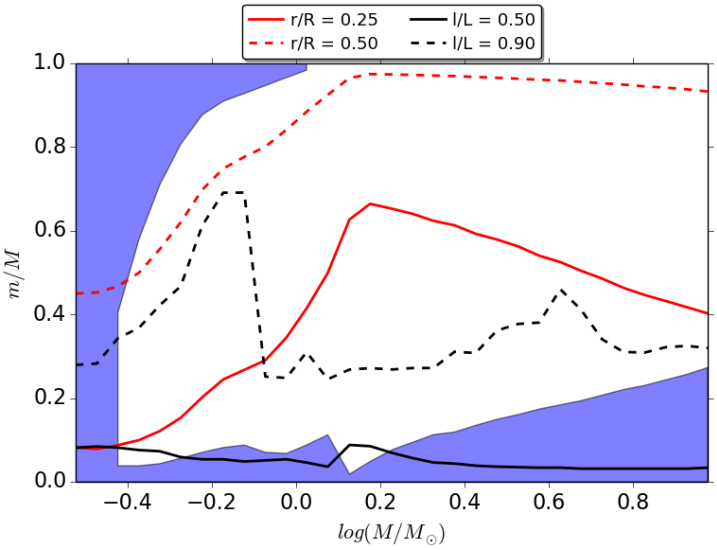

Figure 10: The Kippenhahn diagram at the ZAMS, reproduced via using `MESA`.

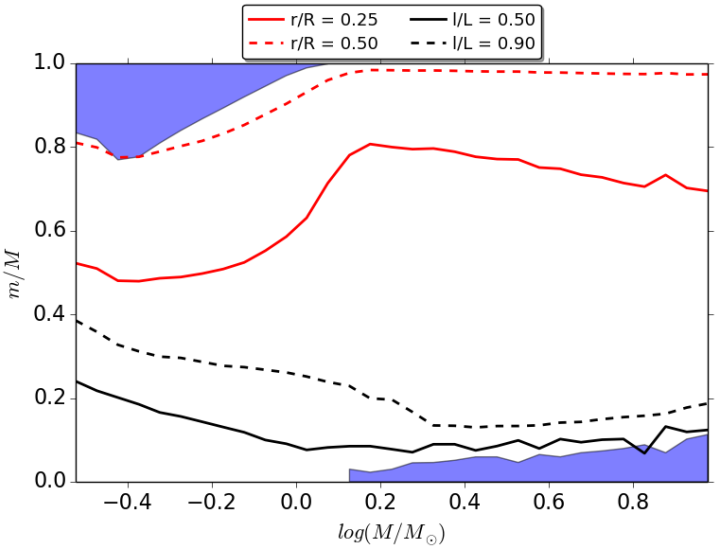

Figure 11: The Kippenhahn diagram at the TAMS, reproduced via using MESA.

5 Hydrogen Profiles

Stellar evolution describes the radical changes which stars undergo throughout their lifetime. The timescales of these processes differ substantially based on the physical process occurring in the stellar interior. Nuclear fusion is the primary energy production process for the majority of a star's life, determining the stellar evolutionary path. This process is highly temperature dependent and thus these reactions occur fastest at the core, resulting in a gradient in the mass fraction of hydrogen throughout the star. This gradient is determined by the current evolutionary state of the star and can be mapped using the hydrogen profile diagram. This diagram is constructed by plotting hydrogen mass fraction ($X(m_H/M)$) against stellar mass fraction (m/M) as shown in Figure 12.

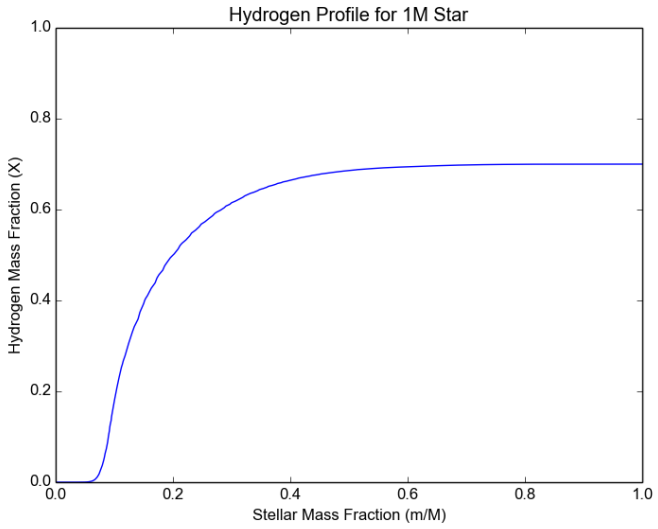

Figure 12: Example hydrogen profile for a $1M_\odot$ star.

We produced hydrogen profiles for $0.8M_\odot$, $1M_\odot$, $1.4M_\odot$, $2M_\odot$ and $5M_\odot$ stellar models at different evolutionary stages, with an initial metallicity of Z = 0.02. These hydrogen profiles can be separated into two groups which are exemplified by the $1M_\odot$ and $5M_\odot$ stellar models included here (Figures 13 and 14). Figure 13(a) shows hydrogen profiles for a $1M_\odot$ stellar model until the depletion of core hydrogen. The first hydrogen profile, represented by the constant hydrogen mass fraction throughout the stellar model, presents the initial distribution of hydrogen before fusion begins. The following five profiles present the gradual depletion of hydrogen in the core with depletion occurring most rapidly at the center. This depletion profile is typical for stars which exhibit a core radiative zone and an outer convective zone, such as the Sun.

Core radiative zones, based on solar observations, are generally assumed to lack core mixing. Thus, helium produced by nucleosynthesis remains where it was produced, with the fastest production rate at the center of the stellar core where the temperature is greatest. This results in the lowest mass fraction of hydrogen at the center of the core, increasing towards the boundary of the convective envelope from which it remains

constant until shell burning begins. The homogenous distribution of hydrogen throughout the shell results from convective mixing.

The vertical discontinuity in the hydrogen profiles of Figure 13(b) at stellar mass fractions of approximately 0.25 and 0.29 represents the convective shell pushing in as the depletion of core hydrogen continues towards the boundary between the radiative and convective zones. The last profile in this figure shows the complete depletion of hydrogen in the stellar core, with a slight decrease in the hydrogen mass fraction of the convective envelope, indicating the beginning of hydrogen shell burning.

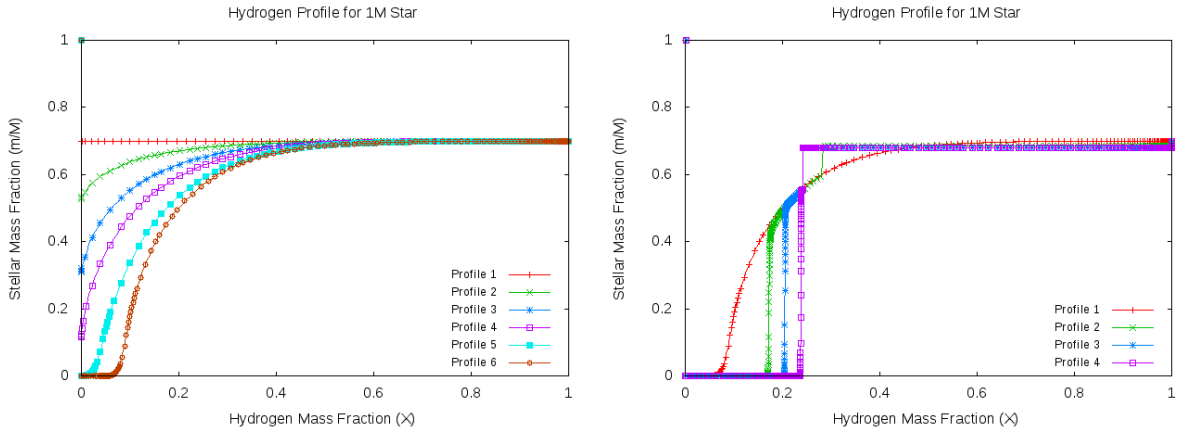

Figure 13: Hydrogen profiles for a $1M_{\odot}$ stellar model (a) until the depletion of hydrogen at the center of the core and (b) after the depletion of central core hydrogen. The first hydrogen profile in (b) is a duplicate of the last profile in (a) and is included as a reference point between the two figures.

The stellar structure of higher mass stars is significantly different to solar mass stars as indicated by the hydrogen profiles of the $5M_{\odot}$ stellar model (Figure 14). The model indicates these stars are composed of a convective core, followed by a radiative zone and a convective outer shell. The convective zones are easily identifiable as convective mixing, which occurs on a much shorter timescale to the stellar evolution, results in a homogenous distribution of hydrogen within the region. As the model is evolved, the hydrogen mass fraction in the core undergoes a uniform reduction. This drop in hydrogen abundance leads to a decrease in opacity in the core, causing it to shrink and the radiative zone to expand inwards.

The last three profiles show the complete depletion of core hydrogen. In profile seven the model has evolved to the point where hydrogen shell burning has begun. The hydrogen distribution within the radiative zone has started to decrease, resulting in the helium core extending beyond that of the smallest convective core. The vertical discontinuity in the last two profiles indicates the boundary between the convective outer shell and radiative zone. The complete depletion of hydrogen within both the convective core and the radiative zone is evident in the final profile.

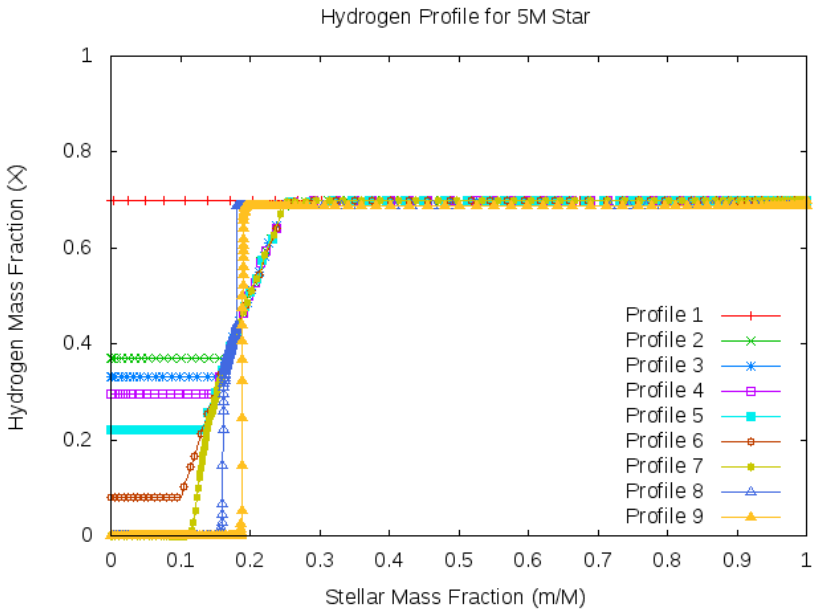

Figure 14: Hydrogen profiles for a $5M_{\odot}$ stellar model.

Acknowledgments

The authors wish to thank to the members of the Stellar Astrophysics Centre at the Aarhus University the organization and funding of the Summer School. ZK is grateful for the financial support from the University Observatory Munich.

References

Çalışkan, Ş. and et al., 2014, *Chemical abundances of the metal-poor horizontal-branch stars CS 22186-005 and CS 30344-033*, Astronomy & Astrophysics, Volume 571, id.A62, 10 pp.

Carraro, G., Monaco, L. and Villanova, S., 2014, *Abundance analysis of red clump stars in the old, inner disc, open cluster NGC 4337: a twin of NGC 752?*, Astronomy & Astrophysics, Volume 568, id.A86, 7 pp.

Carroll, Bradley W. and Ostlie, Dale A., 2007, *An Introduction to Modern Astrophysics*, Addison-Wesley, San Francisco: Pearson, 2nd (International)

Christensen-Dalsgaard J., 2013, *Lecture Notes on Stellar Evolution*

Kippenhahn, R., Weigert, A. 1990, *Stellar Structure and Evolution*, 1st ed., Springer

Kippenhahn, R., Weigert, A., Weiss, A. 2012, *Stellar Structure and Evolution*, 2nd ed., Springer

Mihalas, D. 1978, *Stellar Atmospheres*, 2nd ed., W. H. Freeman, San Francisco.

Palla, F. and Stahler, S. W., 1999, *The Astrophysical Journal*, Volume 525, Issue 2, pp. 772-783

Paxton, B., et al. 2011, *ApJS*, 192,3

Paxton, B., et al., 2013, *ApJS*, 208, 4